Investigative photometry experiments on planar extended-light sources

OPEN ACCESS
IOP Publishing
European Journal of Physics
Eur. J. Phys. **45** (2024) 065301 (19pp)
https://doi.org/10.1088/1361-6404/ad6e44

Investigative photometry experiments on planar extended-light sources

M Campione[1], A Pietropaolo[2] and G Bussetti[3]

[1] Department of Earth and Environmental Sciences, University of Milano - Bicocca, I-20126, Milano, Italy
[2] Nuclear Department, ENEA, I-00044, Frascati (Roma), Italy
[3] Department of Physics, Politecnico di Milano, I-20133, Milano, Italy

E-mail: marcello.campione@unimib.it

Received 13 May 2024, revised 17 July 2024
Accepted for publication 12 August 2024
Published 11 September 2024

Abstract

The inverse-square decay law of the illuminance of a point light source with distance is a common notion of basic optics theory, which is readily demonstrated to be a direct consequence of the propagation of spherical wave fronts with the centre at the light source. It is far less common to address the experimental verification of this law and, even less, to study the illuminance decay with the distance of extended light sources, which somehow represent an unknown topic. We propose a scientific experiment where the light sensor of a smartphone is used to collect illuminance data as a function of the source-to-sensor distance and orientation. Through this procedure, students can realize the limit of validity of the inverse-square law and determine the luminance flux of the chosen point-like light source (e.g. the white LED flashlight of a smartphone). More interestingly, when dealing with extended sources (e.g. the LCD of a laptop displaying a white image) subtle characteristics of the decay trend emerge, particularly for distances lower that the source size. A detailed analysis of these characteristics is presented though a process allowing student engagement in a real scientific investigation, envisaging steps of data acquisition through experimental measurements, model construction on the basis of the observed patterns, and finally model testing. We provide a guided formulation for the general modelling of planar emitters, starting from the theoretical treatment of Lambertian sources. In this way, students are able to quantify the luminous emission also for extended sources and their deviation from a Lambertian behaviour.

Keywords: photometry, extended light source, lux-meter, illuminance decay, lambertian emitter, luminance, emission pattern

1. Introduction

Teachers involved in fundamental physics courses share the common feeling that a serious need is rising to integrate practical experimentation in theoretical courses, to cope with the lack of dedicated spaces and limited budgets for instrumentation [1–5]. During lectures in experimental physics (classical mechanics, thermodynamics, electromagnetism), students learn new concepts and laws, however, the way these laws are discovered and how they can be exploited to be predictive in new experiments is not clear. In a laboratory, current commercial apparatuses and the quality of their software generally give the wrong impression of 'perfect' data acquisition, and students are not able to evaluate the uncertainties and accuracies of the data they collect. The analysis of the experimental results is also difficult because the students are not always in a position to develop critical thinking during their studies. These problems pose limits to the possibility for students to develop modelling skills, representing the most precious outcome of learning, regardless of whether they consist of model evaluation through experimental activities, or model development and analysis through theoretical activities [6]. For this reason, most laboratory activities possess a confirmatory goal and foresee the achievement of a specific result. This feeds the general belief that confirmation represents the primary goal of science learning, while facing a real scientific investigation is just a prerogative of experienced scientists [7]. Moreover, the frustration arising from the obtainment of a non-expected result, added to the desire to be done with the experimental assignment, was demonstrated to engage students in questionable research practices [8].

Our original goal was to offer students an ambitious lab approach that, on the one hand, enforces the possibility of enhancing the conceptual understanding of the practice of model testing, i.e. the evaluation of the degree of appropriateness of an ensemble of models, and, on the other hand, stimulates to debate experimental data in view of developing experimentation skills [8]. In this framework, the *post-mortem* analysis of 'not expected' results is the main driver of this debate, leading to the development of reflective thinking and the belief that the lab activity is not only an exercise of confirmation but allows experiencing how scientists construct knowledge.

In recent years, the principles of the Investigative Science Learning Environment (ISLE) method were purposely formulated to convey this message [9, 10]. ISLE is meant to implement active-learning methods in such a way to guide the students as close as possible to experience scientific processes. This comprises the ability to recognise reproducible patterns in the collected data and from them devising adequate hypotheses, testing them, and finally formulating a prediction. We present here a photometry experiment based on the use of a smartphone light sensor and designed following an ISLE approach. Smartphones are widespread devices among students in secondary school and university, offering a series of sensors integrated in a portable device, which are demonstrated to allow for prompt and accurate measurements of a group of physical quantities [11, 12]. The smartphone camera was used to explore the limits of the thin-lens approximation [13] and to build a DIY spectrometer [14]. The smartphone light sensor was utilized to test Malus's law [15–17], to monitor the circular motion of a light-emitting object [18], to measure the Brewster angle [19], to perform turbidity measurements of sugar solutions [20] and transmittance measurements to verify the

Lambert–Beer law [21–24], and to characterize point-like sources [16, 20, 25, 26] as well as linear sources [27]. By adopting smartphones as measurement instruments, teachers have the potential to design an experimental apparatus, enabling the testing of a physics law and/or the investigation of a phenomenon starting from materials of immediate availability (objects commonly adopted at home or in the classroom) and then ensuring very contained cost. Our experiment aims at the investigation of the properties of planar extended light sources in terms of the luminous intensity emitted and its dependence on the emission direction. On the one hand, this experiment allows the testing of established laws describing the decay of radiation intensity with distance and, on the other hand, an in-depth analysis of the collected data and a guided mathematical modelling allow us to find out unexpected characteristics both of the selected light sources and the employed sensors.

A light source is defined as a device capable of emitting electromagnetic radiation visible to the human eye, i.e. with a wavelength approximately in the range $400 - 700$ nm (and correspondingly frequencies of the order of 10^{15} Hz or 10^3 THz). The light sources differ according to the power emitted in the form of electromagnetic waves, their size, and the direction of their emission. According to the International System, the total luminous flux emitted by a source is defined as lumen (lm). 683 lm corresponds to a power of 1 W, emitted in the form of light radiation with a frequency of 540 THz (perceived as green-yellow light; see the new definition of the units of measurement of the International System promulgated in 2020) [28]. This frequency (corresponding to a radiation propagating in a vacuum with a wavelength of about 555 nm) is taken as a reference, being the one to which the human eye shows maximum sensitivity. Sensitivity progressively decreases until it vanishes towards the lower frequencies of the visible spectral range (red light) and the higher ones (violet light). In order to be able to define the luminosity of a white light source (i.e., composed of a continuous spectrum of visible radiations), it is necessary to integrate the emitted power of all visible radiations weighted by the photopic sensitivity curve [29]. With the term *illuminance*, it is defined as a physical quantity that expresses the luminous flux across a unit surface. The unit of measurement of illuminance is lm m^{-2}, a combination that gives rise to the *lux* (lx). It is natural that for non-collimated, i.e., diverging radiation sources, the illuminance decreases as a function of the distance from the source. In the case of point sources, or for distances from the source much greater than the dimensions of the source itself, the luminous flux is evaluated by integrating the illuminance across a spherical surface, whose centre coincides with the position of the source itself. The luminous flux emitted by the source in all directions (ϕ_0) is transmitted through spherical surfaces with an area equal to $4\pi d^2$, where d is the distance between the surface and the source. Therefore, the decay of illuminance E with distance is expected to follow the relation:

$$E = \frac{\phi_0}{4\pi d^2} \tag{1}$$

In the case of extended sources, the variation of E with the distance d is much more intriguing, depending also on the size and shape of the source [30]. Planar emitters can be approximated as a dense array of point sources uniformly distributed over the surface. The illuminance dependence as a function of the distance from the emitter plane can be evaluated by an integration over the whole surface. For circular surfaces (disk with radius R) with a Lambertian emission pattern, the illuminance decay with distance from the centre of the disc follows the relation [31]:

$$E^{D-L} = \pi L\left[\frac{R^2}{(d^2 + R^2)}\right] \tag{2}$$

where L is the source *luminance* (lm m^2 $Sr^{-1} \equiv$ nit), representing the proper quantity to be used to express the emission properties of extended sources. For a Lambertian emitter, the luminance is independent on the line of sight.

The instrument capable of carrying out illuminance measurements is called a lux-meter and is commonly used to evaluate the illuminance levels of inhabited environments (the normal sources adopted for domestic lighting should reach a luminosity of the order of 300–400 lm for each square meter of surface). The lux-meter installed in smartphones, aimed at optimizing the user's visual experience in relation to the ambient light conditions, is proposed here as a practical instrumentation to allow students to measure the illuminance variation as a function of the distance from freely chosen light sources among a group with point-like characteristics (e.g., the white LED flashlight of a smartphone,) and a group of planar extended sources (e.g., the LCD of a laptop PC or a TV displaying a white image). The experimentation with point-like sources serves to reveal immediately how critical the determination of the illuminance at short distances is, which allows the operator to individuate the validity range of equation (1) and become aware of the possible achievement of the saturation limit of the sensor. Once these aspects are addressed, the student will be able to obtain the best estimate of the luminous flux ϕ_0 [26]. In the case of extended sources, the student must be invited to pay particular care in the mapping of the illuminance data for distances lower than the size of the source, where deviations from the trend predicted by equation (1) are more pronounced. Once data is correctly acquired using the LCD as the source, it is highly probable that the collected pattern significantly deviates from that predicted by equation (2). We provide here the results of a simple mathematical modelling of planar extended sources, showing that not only the size of the source influences the trend, but also the acceptance of the sensor and the level of collimation of the emitted light. By setting an ISLE problem, we describe how guiding students to understand the elements of this modelling, starting from the analysis of qualitative and quantitative patterns observed in the collected data, the formulation of appropriate hypotheses, and the testing of such hypotheses, to finally arrive at the estimation of the properties of the chosen sources and instrumentation in terms of luminance, its dependence on direction, and acceptance of the detector.

2. Description of the experiment

The smartphone to be used as a lux-meter must be equipped with a suitable app enabling the reading of the illuminance. We downloaded and installed *Photometer PRO* by Przemek Pardel, free version (figure 1). The app offers different possibilities that, in principle, can be explored. Here, we focus our attention on the basic operations that can be found in the app utilities which are related to the use of an ambient light sensor, which is separated from the smartphone camera. Illuminance is displayed with the precision on a tenth of a lx and saturates at 10^5 lx. Operators must be wary about the importance in knowing this value. The results of the calibration of smartphone light sensors was recently reported by Tongjan & Sirisathitkul [20]. They showed that smartphones ensure a perfect linear response and precision within 1%; whereas, their accuracy is much affected by the sensitivity to IR radiation, providing for certain source illuminance overestimation as high as 30%.

The position of the light sensor of the smartphone can be located by opening the photometer application and, in a lighted environment, probing the surface of the phone with a fingertip. Before each measurement, the light source and sensor area must be properly

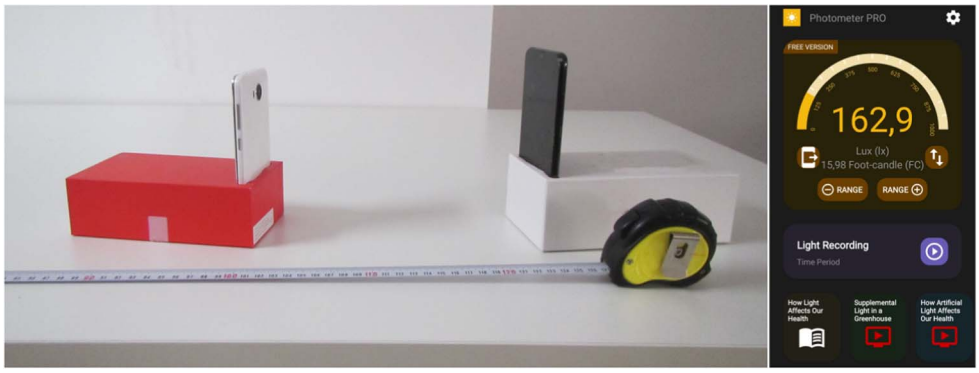

Figure 1. Example of the experimental setup used for illuminance-distance measurements: smartphone boxes are used as support for the source (flashlight, left) and the sensor (photometer, right) is placed on the surface of a table; a meterstick is used to evaluate distances. On the right side, a screenshot of the free version app *Photometer PRO* is displayed.

cleaned. With the aid of a smartphone support, the light sensor is placed on a table i) at the same height as the point-source or ii) at the height level of the centre of the planar extended source (oriented orthogonally to the table plane and displaying a uniform white image). The distance of the sensor from the source must be varied carefully, keeping the plane of the smartphone screen used as a sensor always perpendicular to the sensor-source direction. The sensor-source distance can be measured with a meterstick. The illuminance value must be recorded at each sensor-source distance under dark conditions (i.e., ensuring that light sources in the environment other than that to measure have negligible intensity), and this procedure can be repeated at least 5–6 times to evaluate both the average value and the standard deviation of the illuminance. If the smartphone display is too close to the source screen to allow for the reading of the illuminance, one can use the record function of the software to store the data in a transferrable file.

3. Results and discussion

3.1. Point light source

Figure 2 shows the trend of illuminance E measured by a Huawei P Smart 2019 as a function of distance d from a LED flashlight of a Huawei Y3II (size: 3 mm). Uncertainty on the distance was estimated to be ± 3 mm. This uncertainty is mainly due to the supports used to sustain the two smartphones, which leave a certain amount of backlash to their positioning.

In agreement with equation (1), figure 2(a) shows the rapid decay of E with distance. Figure 2(b) reports E as a function of $1/d^2$ in order to verify the linear trend predicted by equation (1) [25, 26].

Figure 2(b) clearly shows that, if data mapping is sufficiently dense in proximity to the source, for distances less than 30 mm, substantial deviations from the trend expected for a point source are evident. This behaviour is due to the fact that the point-source assumption becomes inadequate when the photometric limit distance is reached, i.e., when the source-sensor distance becomes lower than about ten times the physical size of the source (3 mm $\times$ 10 $=$ 30 mm). The equation of the dashed straight regression line in figure 2(b) is

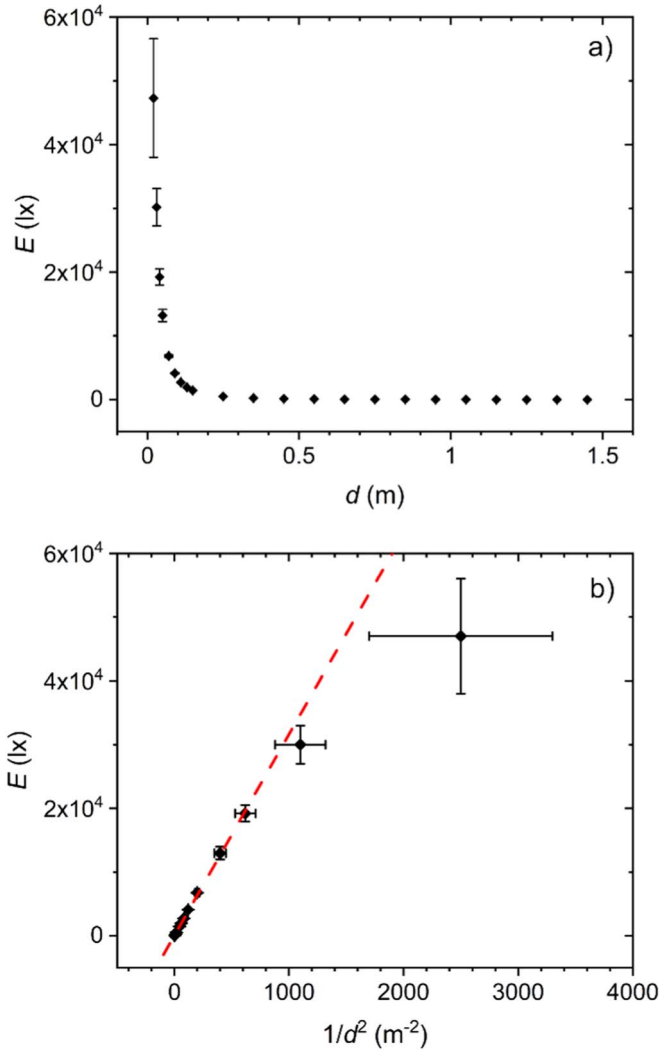

Figure 2. (a) Illuminance as a function of source-sensor distance of a flashlight of a smartphone. The abscissa data uncertainty is within the size of the symbols. (b) Illuminance as a function of $1/d^2$. The dashed red line represents the linear regression of experimental data excluding those at 1100 and 2500 m^{-2} (see the main text for details).

obtained by excluding the data with abscissa higher than 1000 m^{-2} and results in $E = (60 \pm 40)\text{lx} + [(31.5 \pm 0.3)\text{lm}]\dfrac{1}{d^2}$, with a correlation coefficient $R^2 = 0.9988$. From the angular coefficient of the regression line, it is possible to obtain the point source luminous flux. In fact, $(31.5 \pm 0.3)\text{lm} = \dfrac{\phi_0}{4\pi}$, from which we obtain $\phi_0 = 396 \pm 4$ lm. The luminous flux value obtained, of the order of 400 lm, is fully consistent with the expected nominal one for a white LED diode, usually included in the range $200 - 300$ lm per watt [32].

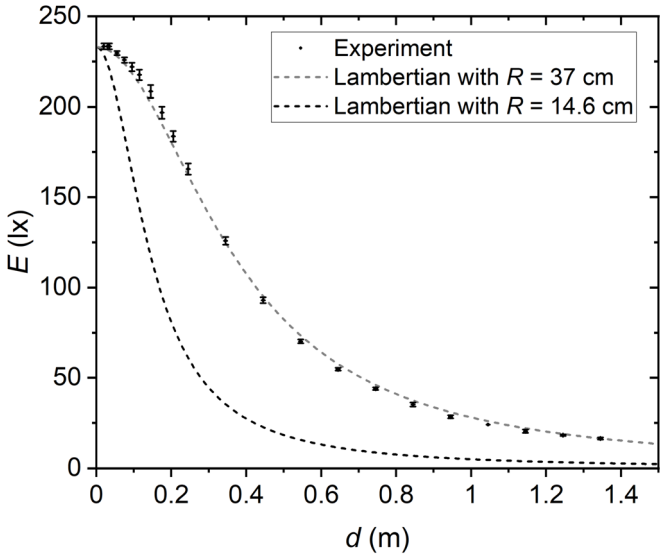

Figure 3. Illuminance as a function of source-sensor distance of a 15″ LCD displaying a uniform white image. The abscissa data uncertainty is within the size of the used symbols. The black dashed curve corresponds to the illuminance calculated for a Lambertian discoidal emitter with radius $R = 14.6$ cm, having the same surface area as that of the 15″ LCD. The grey dashed curve corresponds to the illuminance calculated for a Lambertian discoidal emitter with radius $R = 37$ cm.

3.2. Extended light source

3.2.1. Experimental measurement and identification of qualitative and quantitative patterns.

Figure 2 reveals that, when the point-source approximation becomes too drastic, detected illuminance is lower than expected. In order to investigate the deviation of the illuminance trend in detail, from that which is predicted by equation (1), the mapping of illuminance can be performed using a well-defined planar emitter such as an LCD. Figure 3 shows the trend of illuminance measured as a function of distance from a 15″ LCD (19.5 cm $\times$ 34.5 cm) displaying a uniform white image. The distance uncertainty was estimated to be ± 2 mm.

In the experimental trend displayed in figure 3, one can identify the following relevant patterns: 1) the illuminance as a function of the distance does not follow a simple power law; 2) for distances from the screen below 0.05 m, the illuminance is almost constant, and reaches a maximum at (233 ± 2) lx. This represents a saturation value which is characteristic of the adopted screen and the brightness level; 3) in the distance range $0.05 - 0.2$ m, the illuminance significantly decreases; finally, 4) beyond 0.2 m, the illuminance continues to decrease but with a progressively slower rate. It is evident from figure 3 that E undergoes a continuous variation of its trend with d. It is interesting to note that, for lengths comparable to the screen size (19.5 cm $\times$ 34.5 cm), the decreasing rate seems to reach its maximum.

It is worth comparing the experimental trend with that predicted in the case of a Lambertian emitter [31, 33], expressed by equation (2) (see also passages bringing to equation (A10)): $E^{D-L} = \pi L \left[\dfrac{R^2}{(d^2 + R^2)} \right]$. In accordance with it, the illuminance trend is regulated by two parameters: the screen luminance L and the screen surface area. The screen output can be approximated by that of a disk having the same surface area, i.e. with radius

$R = [(19.5 \times 34.5)/\pi]^{1/2} = 14.6$ cm (see appendix and figure A9)). At low distances, illuminance is predicted to saturate to the value of the screen luminous exitance, πL (lm m^{-2}). If we set $\pi L = (233 \pm 2)$ lx, we obtain $L = (74.2 \pm 0.6)$ nit.

Even though it is possible to verify the saturation behaviour of the illuminance, figure 3 shows that equation (2) highly underestimates the experimental illuminance for the whole range of explored distances.

At this stage of the experiment, students are in the condition of realising that equation (2) is regulated by two parameters, L and R. L is fixed by the saturation value of E measured near the screen surface, whereas R can be considered a fitting parameter. Hence, students can be invited to identify what the effects of changing the value of R are, starting from the actual one. It can be immediately realized that by increasing R, the interpolation of the experimental results improves to a great extent. On the basis of the data reported in figure 3, a good interpolation is obtained by setting $R = 37$ cm, i.e. 2.5 times higher than the actual radius.

3.2.2. Hypotheses formulation for the observed behaviour. The results reported in figure 3 allow the conclusion that LCDs are non-Lambertian emitters. However, their emission is very well reproduced by a Lambertian emitter with substantially larger size. On the other hand, this conclusion assumes that the collected data is not affected by the response of the light sensor, which might be non-ideal.

Hence, to explain this behaviour, two hypotheses can be devised:

(1) The LCD is a non-Lambertian surface, able to 'concentrate' light in a forward direction. The directionality of its emission makes it equivalent to a Lambertian surface with a much larger size.
(2) Following a symmetry principle, the directionality is an effect due to the light sensor, which, similarly to a proximity sensor, is more sensitive to on-axis light intensity, and less sensitive to off-axis light intensity.

The role of directionality is then the main aspect students must recognise to regulate the deviation from a Lambertian behaviour. This directionality can be due both to the emitter and the sensor. Its impact on the measured illuminance is the same.

In order to test the two hypotheses, adequate experiments must be designed. We present below a possible set of experiments and the related modelling scheme.

3.2.3. Investigating the angular response of the photometer. In order to test hypothesis 2), the angular response of the photometer can be investigated by performing illuminance measurements keeping the source-sensor distance fixed and varying the angle θ between the direction normal to the plane of the smartphone-source and that one of the sensor (figure 4). The experiment foresees the employment of a point light source. Figure 4 shows the polar diagram of the illuminance measured as a function of the azimuthal angle $\theta = \sin^{-1}\frac{h}{d}$ for the same source adopted in figure 2, where d is the source-sensor distance and h is that of the source from the optical axis.

The illuminance as a function of angle θ is reported in figure 5(a) on a Cartesian diagram, where, for comparison, the function $E = E_0[\cos^i(\theta)]$ (with $i = 1$, 2, and 3) is also shown. E_0 is the illuminance measured at $\theta = 0°$.

The case with $i = 0$ would correspond to a response of the photometer independent on the incidence angle of the light rays coming from the source, which is unfeasible. The expected response is described by the case with $i = 1$, which takes into account the projection of the sensor active area orthogonally to the line of sight (figure 4(a) and see appendix).

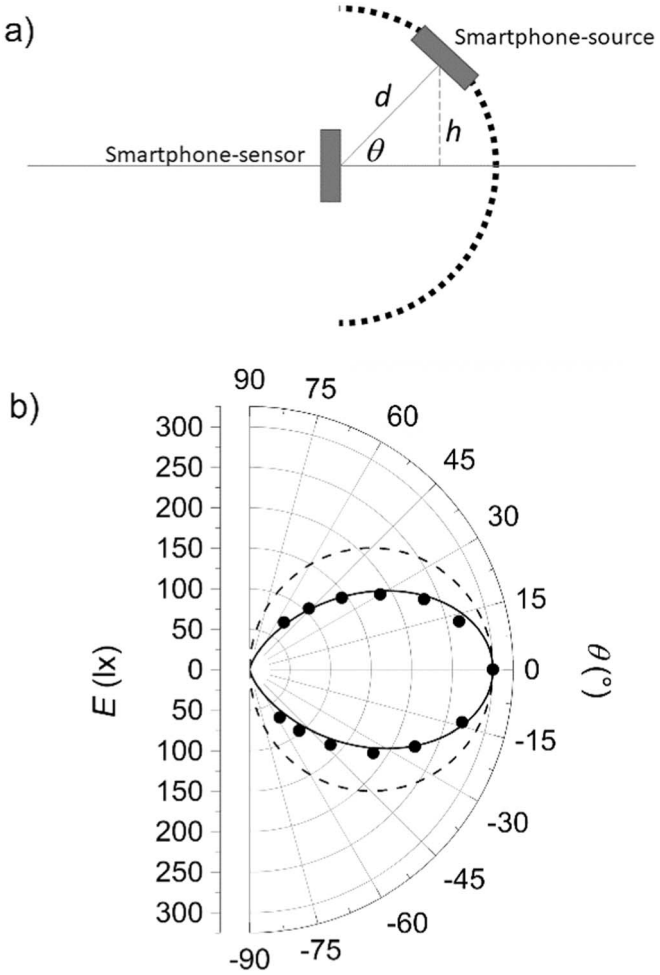

Figure 4. (a) Top-view of the experimental geometry adopted to evaluate the angular response of the lux-meter and (b) the polar diagram of the illuminance measured as a function of the azimuthal angle θ, and at a fixed source-sensor distance of 33.5 cm. The experimental uncertainties are within the size of the adopted symbols. The dashed circle represents the expected response of the photometer since the detector area projected on a plane normal to the sensor-source direction follows the function $E = E_0[\cos(\theta)]$. The black solid line reproduces the function $E = E_0[\cos^3(\theta)]$.

However, as the angle of incidence increases, the experimental illuminance decay is observed to move away substantially from the $i = 1$ curve. The function $E = E_0[\cos^3(\theta)]$ is observed to represent the best approximation of the illuminance angular dependence. This effect is the result of a limited acceptance of the employed photometer. The estimate of its angle of acceptance within the horizontal plane is provided by the width at half maximum of the function, resulting in 75°, in comparison with 120° corresponding to the expected one.

In order to model the effect of a reduced acceptance on the measured illuminance, it is clear that, mathematically, a term of the type $\cos^i(\theta)$ with $i > 1$ must substitute the term $\cos(\theta)$ appearing within the function to integrate over the whole screen surface. The result of this operation is described in the appendix, and provides the result expressed by

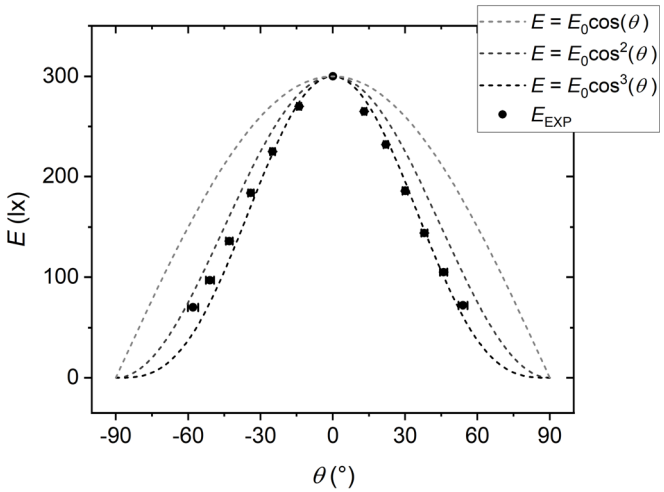

Figure 5. Illuminance (black dots) measured by the sensor of a smartphone as a function of the azimuthal angle (see the main text for details) and at a fixed source-sensor distance of 33.5 cm. The dotted curves represent the trend of the function $E = E_0 \cos^i(\theta)$, with $i = 1, 2, 3$, as displayed by the legend.

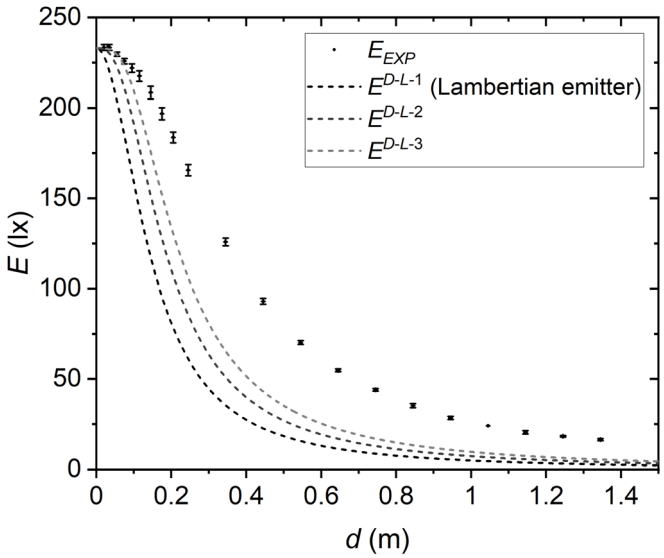

Figure 6. Illuminance versus source-sensor distance of a 15″ LCD displaying a uniform white image (black dots) and illuminance versus source-sensor distance calculated with equation (A13) for a Lambertian emitting disk with radius 14.6 cm.

equation (A13): $E^{D-L-i} = \dfrac{2\pi L}{(1+i)}\left[1 - \dfrac{d^{1+i}}{(d^2+R^2)^{(1+i)/2}}\right]$. Figure 6 shows the illuminance behaviour in accordance with equation (A13) compared with the experimental data (figure 4).

It is evident from figure 6 that, even though all the curves of $E^{D\text{-}L\text{-}i}$, already for distances greater than 0.1 m, still substantially underestimate the experimental data, from a purely

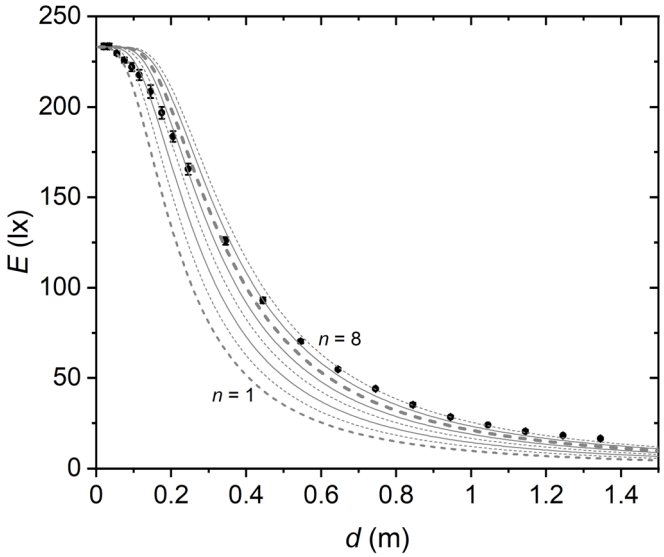

Figure 7. Illuminance as a function of the source-to-sensor distance of a 15″ LCD displaying a uniform white image (black dots), and illuminance as a function of the source-to-sensor distance calculated with equation (A15) with $i = 3$ and for an emitting screen consisting of a distribution of light sources with progressively more collimated emissions (dashed lines with $n = 1, 2, \ldots, 8$; thicker dash for $n = 1$ (Lambertian screen) and $n = 6$).

mathematical point of view, powers of the cosine with $i > 1$ improve the interpolation of the experimental trend. Moreover, this procedure suggests that powers of the cosine with $i > 3$ would further improve the interpolation. However, this occurrence is unjustifiable for the adopted sensor.

To get around this bottleneck, one has to realise that a directionality term of the type $\cos^i(\theta)$ can be applied not only to the sensor, but also to the emitter. This translates into a non-Lambertian emission [34–37]. Indeed, in a Lambertian emitter, the luminance is independent on the emission direction, whereas deviation from a Lambertian behaviour can be expressed by a luminance angular dependence of the type: $L = L_0 \cos^{(n-1)}(\varphi)$ (the case $n = 1$ representing that of a Lambertian emitter), which mathematically brings us to the same result expressed by equation (A13).

3.2.4. Investigating the directionality of the screen emission. In order to test hypothesis 1), we can adopt a generalisation of equation (A13), in which we indicate an additional exponent n quantifying the emission directionality. This brings us to equation (A15): $E^{D-i,n} = \dfrac{2\pi L_0}{(i+n)}\left[1 - \dfrac{d^{i+n}}{(d^2+R^2)^{(i+n)/2}}\right]$ (see appendix).

Figure 7 shows the trend predicted by equation (A15) (with $i = 3$), compared with the experimental data.

As the light source collimation increases (i.e., as the value of n increases), the plateau becomes more pronounced, while the decay with distance becomes less steep. Within the limits of the proposed model, we consider the $n = 6$ curve as the best interpolation of our experimental data. As a consequence, this result validates a model where light emission from

the LCD is partially collimated. The level of collimation can be estimated from the width at half maximum of the curve, $E = E_0 \cos^6(\theta)$, being equal to 55°.

From the saturation value (233 ± 2) lx, we can obtain from equation (A15) the frontal luminance $L_0 = \frac{(i+n)}{2\pi} E_{sat}^{D-i,n}$. For $i = 3$ and $n = 6$, $L_0 = (334 \pm 3)$ nit. Note that this luminance level is much higher than the one estimated in section 3.2.1, being (74.2 ± 0.6) nit. Indeed, this latter represents an average value of a quantity which reaches its maximum value along a direction orthogonal to the screen surface.

By comparing figures 3 and 7, one might observe that a better interpolation of experimental data is achieved using equation (2) rather than equation (A15). This can be attributed to the fact that even though the cosine powers allow the introduction, with a very simple mathematical function, of the directionality both in the source emission and in the sensor detection, the actual emission(acceptance) pattern of the source(sensor) might not be cosinusoidal, but probably elliptic [38].

As a countercheck, one can verify if our emission model is in agreement with technical data available for the LCD. Actually, it was recently reported that the partial collimation of the LED light used in the backlighting of LCD brings significant advantages in terms of contrast ratio and the reduction of colour shift with varying viewing angle [38–40]. On the other hand, a better trade-off can be obtained with displays adopting active-matrix organic light-emitting diodes (AMOLED). By testing these screens with the described procedure, one might expect to detect a relatively lower level of illuminance but the illuminance trend with distance might be consistent with a much more constant illuminance level with the viewing angle (Lambertian behaviour) [41, 42].

Finally, we observe that, as the curves shown in figure 7 do not show unique features at a distance equal to the diameter of the screen (about 0.3 m), the trend of the illuminance with distance is the result of a combined effect produced by the angular dependence of the photometer acceptance and the luminance of the light source.

4. Students' reactions and recurrent caveats

The illustrated experiment was tested in two classes of first-year undergraduate students, one in an Engineering School and one in a Science School, composed by a group of twenty experimenters each. A common reaction of students who performed the experiment is actually the impression of facing an 'unexpected' result. With the term unexpected it is meant that, in regards particularly to the measurements performed on extended light sources, no single equation is available to reproduce experimental results as in other more common experiments. The results seem to totally deviate from a theorized behaviour, giving the feeling that no tool is available for their interpretation. Actually, the behaviour of the extended sources is hardly discussed in physics courses [30], and results appear as extremely source-dependent. With the scope to guide students along a research-like path for the interpretation of their results, after the individuation of qualitative and quantitative patterns of the illuminance trend as a function of distance (section 3.2.1), we invited them to test known models of planar emitters (equation (2)). Students recognised that the available models for Lambertian emitters apparently fail to reproduce the measured trend and readily realised that LCDs behave like Lambertian emitters with a substantially larger size. At this stage, students were invited to devise a hypothesis to explain the observed behaviour (section 3.2.2). Most of them realised that LCDs behave like 'shrunk' Lambertian sources, providing the same emitted intensity of a larger screen but concentrated along a frontal direction. However, understanding that this brings to the same effects of a reduced acceptance of the sensor appeared to be more difficult.

To test the devised hypotheses, the angular response of the lux-meter was then explored (section 3.2.3), and we mathematically showed how this response can be incorporated within known laws, underlying that the same mathematical result is accomplished by assuming directional emission. With the modified mathematical model, students determined the acceptance level of their light sensor, the collimation level of their LCD and its frontal luminance. We underline that no fitting procedure was recommended; model testing is undertaken by the manual variation of the free parameters.

We noted that most students expressed difficulties in reproducing a polar plot. On this basis, we explicitly invite teachers to stress the importance of this measurement step and to guide students to get familiar with the management of polar plots.

By analysing the range of student results, we realized that there is another critical step of the measurement procedure: students often fail to map near-source values of illuminance. Their typical behaviour is that of mapping the illuminance at distances that are multiple to a fixed interval. As a consequence, the deviation of illuminance as a function of $1/d^2$ in the proximity of point sources (figure 2) and the saturation of the illuminance in proximity of extended planar sources (figure 3) cannot be visualized, missing the fundamental characteristics that distinguish extended sources from point-like ones. In relation to that, since illuminance increases rapidly by approaching the source, students must be aware of the saturation value of their lux-meter, which might differ from smartphone to smartphone. On the contrary, sensitivity and acceptance are rather uniform among devices [20].

As stated above, this experiment allows students to witness unexpected behaviour, which is represented by the interruption of the increase of illuminance while approaching an extended source. This measurement is even more surprising if undertaken after that involving point-like sources, which, regardless their tiny dimension, make the illuminance explode for short distances. The experimental session is undertaken by ensuring dark conditions, which makes the measurement experience even more exciting. The experiment also stimulates in students the desire to compare different screens, giving a sense to possess a solid methodology to test, in terms of intensity and divergence level, the quality of the monitors adopted in everyday life.

5. Conclusions

LCDs represent useful models of planar emitters, a subject traditionally overlooked within programmes of physics experimentation. The measurement of the illuminance as a function of distance from a LCD highlighted the presence of unique patterns, with substantial differences in respect of the response of Lambertian sources, requiring the formulation of a predictive model. Assuming a significant role played by the angular acceptance of the photometer and angular emission of the light source, the explanation of the experimental illuminance decay behaviour is possible. Using the light sensor of a smartphone, the luminous flux of a point-like source and the luminance of an extended planar source can be estimated with an accuracy within 2%.

The described experiment represents an example of application of the ISLE principles, proving that a correct approach allows the acquisition of data of scientific value even though adoptingimmediately available instruments and rustic apparatuses. This requirement is basilar for experiencing not only a simple confirmation of established models, but a thorough predictive modelling process of the observed phenomena though guided critical reflections.

Data availability statement

All data that supports the findings of this study is included within the article (and any supplementary files).

Appendix : Influence of the photometer acceptance and directionality of the emission pattern on illuminance measurements

We can assume that the extended planar source is represented by a continuous and uniform radiating rectangular surface with area $A = a \times b$ (6.73×10^{-2} m^2 for a 15' LCD) in the x-y plane (a and b represent the dimension of the sides of a 16:9 screen), and the centre at the origin of the reference system. Each infinitesimal flat portion of the screen of extension $\delta x \delta y$ can be considered an isotropic point emitter, radiating a flux $\delta\phi_0^{P-I}$ proportional to the overall flux ϕ_0: $\delta\phi_0^{P-I} = \frac{\phi_0}{A}\delta x \delta y$. The related infinitesimal luminous flux areal density at a distance d along the z-direction (sensor axis) follows the law $\delta\Phi^{P-I} = \dfrac{\delta\phi_0^{P-I}}{2\pi(x^2 + y^2 + d^2)}$. The illuminance can be obtained after a proper integration over the entire emitting surface, and considering that at an angle φ , i.e. the angle between the surface element normal and the direction of observation (figure A1), the detector receives a flux reduced by a factor $\cos(\varphi) = \dfrac{d}{(x^2 + y^2 + d^2)^{1/2}}$:

$$E^{P-I} = \int_{-a/2}^{a/2}\int_{-b/2}^{b/2} \frac{\phi_0}{2\pi A}\frac{d}{(x^2 + y^2 + d^2)^{3/2}}\delta x \delta y \tag{A1}$$

bringing us to:

$$E^{P-I} = \frac{2\phi_0}{\pi A}\mathrm{atan}\left[\frac{ab}{4d\left(\left(\frac{a}{2}\right)^2 + \left(\frac{b}{2}\right)^2 + d^2\right)^{1/2}}\right] \text{[Rectangular isotropic emitter].} \tag{A2}$$

To simplify the calculus, without changing the physical problem, we assume a circular (non-rectangular) emitting surface with radius R, but having the same area A ($R = 1.46 \times 10^{-1}$ m for a 15' LCD). Under this new geometrical conditions, considering that a ring contributes to a fraction of the total intensity of light emitted equal to $\delta\phi_0^r = \dfrac{\phi_0}{A}2\pi r \delta r$, where $2\pi r \delta r$ represents the infinitesimal area of a ring of radius r and thickness δr, the luminous flux areal density of an isotropic concentric emitting ring of radius r of infinitesimal thickness is $\delta\Phi^{r-I} = \dfrac{\delta\phi_0^r}{2\pi(r^2 + d^2)}$ (figure A1).

By using the relation $\cos(\varphi) = \dfrac{d}{(r^2 + d^2)^{1/2}}$, the illuminance value measured by the photometer at a distance d along the axis of a ring source of radius r is:

$$\delta E^{r-I} = \frac{\delta\phi_0^{r-I}}{2\pi}\frac{d}{(r^2 + d^2)^{3/2}}. \tag{A3}$$

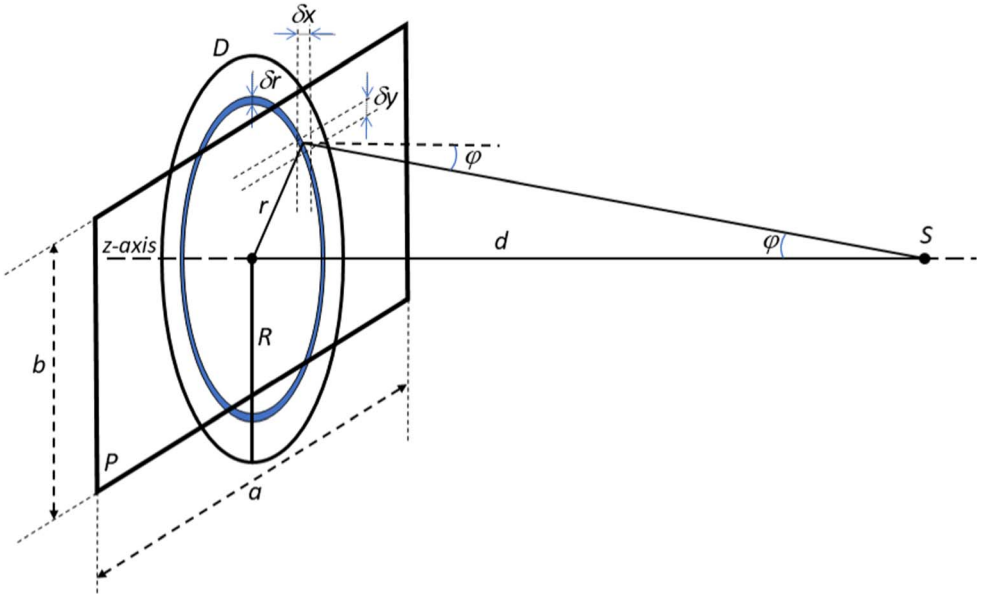

Figure A1. Schematics showing the geometry for deriving equations (A2) and (A5). A luminous plane (P) of sides a and b is separated by a distance d from the light sensor (S). An infinitesimal plane element of area $\delta x\delta y$ illuminates the sensor along a direction forming an angle φ with the disc surface normal. The luminous plane is approximated by a concentric luminous disc (D) of radius $R = [(a \times b)/\pi]^{1/2}$. An infinitesimal concentric ring of radius r and thickness δr illuminates the sensor along a direction forming an angle φ with the disc surface normal.

Hence, the illuminance produced from the entire isotropic disk results in:

$$E^{D-I} = \int_0^R \frac{\phi_0}{A}\frac{d}{(r^2 + d^2)^{3/2}} r\delta r \tag{A4}$$

bringing us to:

$$E^{D-I} = \frac{\phi_0}{A}\left[1 - \frac{d}{(d^2 + R^2)^{1/2}}\right] \text{[discoidal isotropic emitter]}. \tag{A5}$$

In the case of a Lambertian emitter [31], the luminous flux areal density displays an angular decay in accordance with the law:

$$\delta\Phi^{r-L} = \frac{\delta\phi_0^r}{2\pi(r^2 + d^2)}\cos(\varphi). \tag{A6}$$

The illuminance measured by the photometer modifies into:

$$\delta E^{r-L} = \frac{\delta\phi_0^r}{2\pi(r^2 + d^2)}\frac{d^2}{(r^2 + d^2)} = \frac{\delta\phi_0^r}{2\pi}\frac{d^2}{(r^2 + d^2)^2}. \tag{A7}$$

The illuminance produced from the entire Lambertian disk results in:

$$E^{D-L} = \int_0^R \frac{\phi_0}{A}\frac{d^2}{(r^2 + d^2)^2} r\delta r \tag{A8}$$

which, after integration, brings us to:

$$E^{D-L} = \frac{\phi_0}{2A}\left[\frac{R^2}{(d^2 + R^2)}\right]. \tag{A9}$$

Equation (A9) represents a special case of the more general equations obtained by Ivchenko [33] and assuming the disc luminance $L = \frac{\phi_0}{2\pi A}$:

$$E^{D-L} = \pi L\left[\frac{R^2}{(d^2 + R^2)}\right] \text{[discoidal Lambertian emitter]}. \tag{A10}$$

In accordance with the results illustrated in figure 5, the effect of a reduced acceptance is that to introduce a factor of $\cos^i(\varphi) = \left[\frac{d}{(r^2 + d^2)^{1/2}}\right]^i$ in the integrand of equation (A8), which can be rewritten in the general form:

$$E^{D-L-i} = \int_0^R \frac{\phi_0}{A}\frac{d^{1+i}}{(r^2 + d^2)^{(3+i)/2}} r\delta r; \tag{A11}$$

bringing us to:

$$E^{D-L-i} = \frac{\phi_0}{(1 + i)A}\left[1 - \frac{d^{1+i}}{(d^2 + R^2)^{(1+i)/2}}\right]; \tag{A12}$$

or, equivalently:

$$E^{D-L-i} = \frac{2\pi L}{(1 + i)}\left[1 - \frac{d^{1+i}}{(d^2 + R^2)^{(1+i)/2}}\right]$$
[discoidal Lambertian emitter with reduced acceptance]. (A13)

It is worth noting that equation (A10) and equation (A13) correctly approximate to $E = \frac{\phi_0}{2\pi d^2}$ for $d \to \infty$.

In the case of a non-Lambertian source, we can assume that the ensemble of the point sources emit intensities preferentially along an orthogonal direction, following an angular dependence described by the function $\cos^n(\varphi) = \left[\frac{d}{(r^2 + d^2)^{1/2}}\right]^n$ $(n > 1)$ [34–37]. This modifies the luminance in accordance with the relation $L = L_0 \cos^{(n-1)}(\varphi)$, and the illuminance according to the function $\delta E^r = \frac{\delta\phi_0^r}{2\pi}\frac{d^{i+n}}{(r^2 + d^2)^{(2+i+n)/2}}$, which is obtained by multiplying the second member of equation (A6) by the factor $\cos^n(\varphi) = \left[\frac{d}{(r^2 + d^2)^{1/2}}\right]^n$.

Following the same integration steps as before, we obtain:

$$E^{D-i,n} = \frac{\phi_0}{(i + n)A}\left[1 - \frac{d^{i+n}}{(d^2 + R^2)^{(i+n)/2}}\right]; \tag{A14}$$

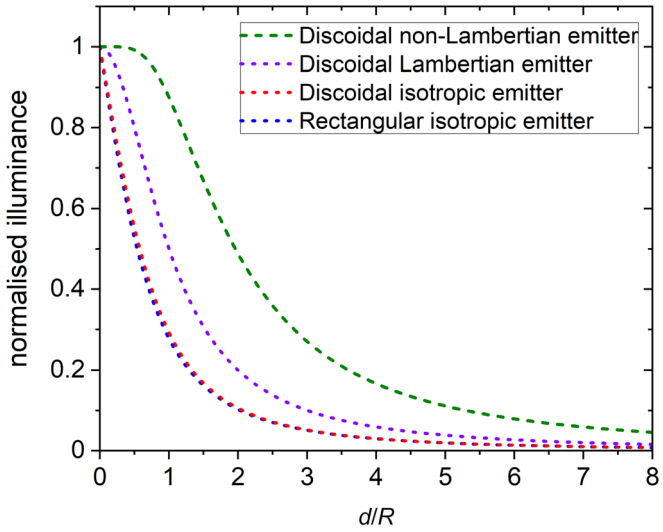

Figure A2. Normalised illuminance as a function of relative distance predicted by equation ((A2), rectangular isotropic emitter with sides $a \times b = \pi R^2$), ((A5), discoidal isotropic emitter with radius R), ((A10), discoidal Lambertian emitter with radius R), ((A15), discoidal non-Lambertian emitter with with radius R setting $i = 3$ and $n = 3$).

or, equivalently:

$$E^{D-i,n} = \frac{2\pi L_0}{(i+n)}\left[1 - \frac{d^{i+n}}{(d^2+R^2)^{(i+n)/2}}\right]$$

[discoidal non−Lambertian emitter with reduced acceptance]; (A15)

which still approximates to $E = \dfrac{\phi_0}{2\pi d^2}$ for $d \to \infty$.

Figure A2 shows the comparison of the illuminance trend with the distance calculated with equations (A2), (A5), (A10) and (A15). Normalised illuminance is expressed with the ratio $E/E_{d=0}$, whereas relative distance is the ratio d/R, where R is the radius of the actual discoidal emitter or the radius of a discoidal emitter having the same area of an actual rectangular emitter. It is worth noting that the two curves comparing the response of two isotropic emitters having the same area but different shape (discoidal and rectangular) are virtually identical.

ORCID iDs

M Campione https://orcid.org/0000-0001-5627-6186
A Pietropaolo https://orcid.org/0000-0003-2554-6985
G Bussetti https://orcid.org/0000-0001-8556-8014

References

[1] Bussetti G, Campione M and Pietropaolo A 2022 *Sperimentare la Fisica* vol 1 (UTET Università)
[2] Searle G F C 2014 *Experimental Physics* (Cambridge University Press)

[3] Leo W R 1994 *Techniques for Nuclear and Particle Physics Experiments* (Springer Berlin Heidelberg) (https://doi.org/10.1007/978-3-642-57920-2)
[4] Moore J H, Davis C C and Coplan M A 2009 *Building scientific apparatus* IV (Cambridge University Press) (https://doi.org/10.1017/CBO9780511609794)
[5] Kraftmakher Y 2014 *Experiments and Demonstrations in Physics* (World Scientific) (https://doi.org/10.1142/8618)
[6] Hestenes D 1992 Modeling games in the newtonian world *Am. J. Phys.* **60** 732–48
[7] Berry M and Popescu S 2023 Discovery experiments and demonstration experiments *Europhys. News* **54** 10
[8] Smith E M, Stein M M and Holmes N G 2020 How expectations of confirmation influence students' experimentation decisions in introductory labs *Phys. Rev. Phys. Educ. Res.* **16** 010113
[9] Etkina E 2023 When learning physics mirrors doing physics *Phys. Today* **76** 26–32
[10] Etkina E and Van H A 2007 Investigative science learning environment—a science process approach to learning physics abstract : table of contents *Res. reform Univ. Phys.* **1** 1–48
[11] Monteiro M and Martí A C 2022 Resource Letter MDS-1: mobile devices and sensors for physics teaching *Am. J. Phys.* **90** 328–43
[12] Sirisathitkul Y and Sirisathitkul C 2023 Smartphones as smart tools for science and engineering laboratory: a review *Iraqi J. Sci.* **64** 2240–9
[13] Sullivan M C 2022 Using a smartphone camera to explore ray optics beyond the thin lens equation *Am. J. Phys.* **90** 610–6
[14] Khandelwal A, Leong T K, Yang Y, Wee L K, García Clemente F J, Venkatesan T and Jani H 2022 Modern physics demonstrations with diy smartphone spectrometers *Phys. Educ.* **4** 2250003
[15] Monteiro M, Stari C, Cabeza C and Martí A C 2017 The polarization of light and malus' law using smartphones *Phys. Teach.* **55** 264
[16] Diaz-Melían V L, Rodŕiguez L A, Pedroso-Camejo F, Mieres J, De Armas Y, Batista-Leyva A J and Altshuler E 2019 Optics undergraduate experiments using smart (and not so smart) phones *Rev. Cuba. Fis.* **36** 4–7
[17] Çolak İ Ö and Erol M 2020 Realization of polarization and malus's law using the smartphones *J. Pendidik. Fis. Indones.* **16** 9–13
[18] Kapucu S 2019 Discovering quantities of circular motion of a light-emitting toy train using a smartphone light sensor *Phys. Teach.* **57** 480–2
[19] Chiang C-M and Cheng H-Y 2019 Use smartphones to measure Brewster's angle *Phys. Teach.* **57** 118–9
[20] Tongjan N and Sirisathitkul C 2020 Accuracy and precision of smartphones in measurements of illuminance and liquid turbidity *Rev. Cuba. Fis.* **37** 131–4
[21] Onorato P, Gratton L M, Polesello M, Salmoiraghi A and Oss S 2018 The beer–lambert law measurement made easy *Phys. Educ.* **53** 035033
[22] Colţ M, Radu C, Toma O, Miron C and Antohe V A 2020 Integrating smartphone and hands-on activities to real experiments in physics *Rom. Reports Phys.* **72** 905
[23] Malisorn K, Wicharn S, Plaipichit S, Pipatpanukul C, Houngkamhang N and Puttharugsa C 2020 Demonstration of light absorption and light scattering using smartphones *Phys. Educ.* **55** 015012
[24] Onorato P, Rosi T, Tufino E, Caprara C and Malgieri M 2021 Using smartphone cameras and ambient light sensors in distance learning: the attenuation law as experimental determination of gamma correction *Phys. Educ.* **56** 045007
[25] Vieira L P, Lara V O M and Amaral D F 2014 Demonstration of the inverse square law with the aid of a tablet/smartphone *Rev. Bras. Ensino Fis.* **36** 3505
[26] Sans J A, Gea-Pinal J, Gimenez M H, Esteve A R, Solbes J and Monsoriu J A 2017 Determining the efficiency of optical sources using a smartphone's ambient light sensor *Eur. J. Phys.* **38** 025301
[27] Salinas I, Giménez M H, Monsoriu J A and Castro-Palacio J C 2018 Characterization of linear light sources with the smartphone's ambient light sensor *Phys. Teach.* **56** 562–3
[28] Martin-Delgado M A 2020 The new SI and the fundamental constants of nature *Eur. J. Phys.* **41** 063003
[29] Sears F W 1958 *Optics* (Addison-Wesley Publishing Company)
[30] Grebe-Ellis J and Quick T 2023 Soft shadow images *Eur. J. Phys.* **44** 045301

[31] Bunch R M 2021 *Optical Systems Design Detection Essentials* ed R Barry Johnson (IOP Publishing) (https://doi.org/10.1088/978-0-7503-2252-2)
[32] Cho J, Park J H, Kim J K and Schubert E F 2017 White light-emitting diodes: history, progress, and future *Laser Photon. Rev.* **11** 1600147
[33] Ivchenko V 2021 Extended versus point light source: where does the difference in the illuminance exist? *Rev. Mex. Fis.* E **18** 127–30
[34] Jannson T, Arik E, Bennahmias M, Nathan N, Wang S, Lee K, Yu K and Poliakov E 2006 Performance metrics for integrated lighting systems *SPIE Proc. Defense, Secur. Cockpit, Futur. Displays II* **6225** 62251E
[35] Jannson T P, Kupiec S A, Kostrzewski A A, Spariosu K, Mintzer D T, Rud M, Tengara I and Vasiliev A A 1997 Phase-space formalism and ray- tracing modeling of photometric quantities *SPIE Proc. Photom. Eng. Sources Syst.* **3140** 36–47
[36] Jannson T P and Bennahmias M J 2004 Phase space and radiometric ray tracing *SPIE Proc. Defense, Secur. Cockpit Displays* **5443** 229–37
[37] Bennahmias M, Arik E, Yu K, Voloshenko D, Chua K, Pradhan R, Forrester T and Jannson T 2007 Modeling of non-Lambertian sources in lighting applications *SPIE Proc. Seventh Int. Conf. Solid State Light* **6669** 66691A
[38] Moreno I and Sun C 2008 Modeling the radiation pattern of LEDs *Opt. Express* **16** 1808
[39] Teng T-C, Sun W-S, Tseng L-W and Chang W-C 2013 A slim apparatus of transferring discrete LEDs' light into an ultra-collimated planar light source *Opt. Express* **21** 26972
[40] Berteloot B, Beeckman J, Stuyven G, Vermeirsch K, Blomme T and Neyts K 2020 Highly collimated backlight for liquid crystal displays *Digest of Technical Papers - SID International Symposium* vol 51 (Blackwell Publishing ltd) 1120–3
[41] Okutani S, Kobayashi M and Ibaraki N 2006 Quantitative evaluation of display characteristics of AMOLED displays *J. Soc. Inf. Disp.* **14** 1119
[42] Kim Y, Chung K, Lim J and Kwon O K 2023 A highly uniform luminance and low-flicker pixel circuit and its driving methods for variable frame rate AMOLED displays *IEEE Access* **11** 74301–11